Correlated Microscopic Observations of Arterial Responses to Intravascular Stenting

K. A. Robinson
Emory University School of Medicine

G. Roubin
Emory University School of Medicine

S. King
Emory University School of Medicine

R. Siegel
Emory University School of Medicine

G. Rodgers
Baylor University School of Medicine

See next page for additional authors

Follow this and additional works at: https://digitalcommons.usu.edu/microscopy

Part of the Life Sciences Commons

Correlated Microscopic Observations of Arterial Responses to Intravascular Stenting

Authors

K. A. Robinson, G. Roubin, S. King, R. Siegel, G. Rodgers, and R. P. Apkarian

CORRELATED MICROSCOPIC OBSERVATIONS OF ARTERIAL
RESPONSES TO INTRAVASCULAR STENTING

K.A. Robinson[1]*, G. Roubin[1], S. King[1], R. Siegel[1], G. Rodgers[2], R.P. Apkarian[3]

[1]Emory University School of Medicine, Atlanta, Georgia
[2]Methodist Hospital and Baylor University
School of Medicine, Houston, Texas
[3]Yerkes Regional Primate Research Center of
Emory University, Atlanta, Georgia

Abstract

Percutaneous catheter implantation of intravascular stent prostheses has emerged as a novel clinical adjunct to balloon angioplasty in the treatment of obstructive atherosclerotic vascular disease. We have examined the cellular and subcellular responses to stenting in the coronary arteries of the dog and pig (both normal and atherosclerotic), and in the iliac arteries and aorta of the atherosclerotic rabbit, using scanning electron, transmission electron, and light microscopies. Stenting in these models resulted in a thrombotic reaction ranging from mild to severe, depending on species and antithrombotic therapy. Subsequent organization of thrombotic material with hyperplasia of smooth muscle and inflammatory cells, luminal recovering with endothelial or pseudoendothelial cells, and atrophy of the tunica media led to incorporation of the prosthesis into the arterial wall. Endothelial or pseudoendothelial cells were observed adherent to the prosthesis as early as one day after placement, and regeneration of a confluent periluminal cell layer occurred within 2 to 4 weeks. Persistent ultrastructural abnormalities of the periluminal cell layer were seen as late as 2 years after stenting, but the intimal hyperplastic response appeared limited.

*Address for correspondence:
Keith A. Robinson
Suite F606
Emory University Hospital
1364 Clifton Road, N.E.
Atlanta, Georgia, 30322
Phone number: (404) 727-4677.

Introduction

Arterial angioplasty by balloon catheter has recently been applied clinically in the treatment of both peripheral and coronary obstructive atherosclerosis (9,12). Even more recently, catheter placement of intravascular prostheses (stents) has been applied as an adjunct to angioplasty, particularly in cases of postprocedural arterial collapse and closure, or in the treatment of recurrent arterial stenosis (38). The histologic responses to angioplasty in both humans and experimental animal models have been documented (3,4,40,45,50). The mechanisms of luminal enlargement by this technique include stretching of the media and adventitia, plaque fracture, and plaque dehiscence. An inevitable but undesirable consequence of angioplasty is partial to total endothelial denudation. Acute vessel collapse can occur when separated "flaps" of arterial intima occlude the lumen after deflation and removal of the balloon catheter. In such cases, stents can then be implanted to mechanically maintain a patent lumen.

Recurrence of the atherosclerotic stenosis is observed in approximately 30% of cases following balloon angioplasty (24). This phenomenon, termed restenosis, is believed to result primarily from the proliferation of smooth muscle cells (SMC) from the arterial media, under the influence of mitogens derived from platelets and leukocytes (2,14,23,35). These circulating cells adhere to exposed subendothelium, and plaque dehiscence facilitates their access to the deeper arterial layers. Thrombus formation and organization along with gradual fibroproliferative luminal narrowing then lead to lesion recurrence. Intravascular stents may inhibit the post-angioplasty restenosis phenomenon by several mechanisms, including improvement of laminar blood flow, reduction of blood flow turbulence and stasis, improvement in arterial geometry, and restriction of

access of platelets and leukocytes to deeper arterial layers by the tacking of intimal flaps.

Several groups of investigators have described the clinical and experimental results of intraarterial stenting using prostheses of various designs (10,33,36,37,38,49). However, there are few reports in the literature which provide detailed and correlated documentation of the arterial cellular and subcellular interspecies healing responses to stenting. Arterial response to microsurgical needle placement (1), vascular grafting (7,8,13,15,26,28,30), balloon catheter injury (17,19,31,41), and other forms of vascular trauma (32,34,46) has been assessed from scanning electron micrographs and this methodology was thought to provide the means to observe intravascular stent placement and response. Accordingly, we have examined the arterial responses to placement of an intravascular stent in three animal models using scanning electron microscopy (SEM), transmission electron microscopy (TEM), and conventional light microscopy. Particular emphasis was placed on assessment of the endothelial cell (EC) response to stenting, with secondary emphasis on early and late thrombotic consequences and intimal fibrotic and inflammatory reactions. These three modes of microscopy were used to provide complete and correlative observations of both the luminal surfaces and abluminal arterial tissues.

Materials and Methods

Stents were placed as a primary intimal injury in the left anterior descending or left circumflex coronary arteries of 39 normal mongrel dogs (25-35 kg) under pentobarbital anesthesia via a femoral arteriotomy, using standard coronary artery catheterization techniques. Eight normal and eight atherosclerotic miniature swine (30-60 kg) were also instrumented in this fashion, using halothane anesthesia. Atherosclerosis was induced in the coronary arteries of miniature swine by feeding a diet enriched with 2% cholesterol, 15% fat, and 1.5% sodium cholate, combined with endothelial denudation of a segment of the coronary artery. Thus the stenting procedure, performed 5 months later, was a secondary intimal injury. For long-term studies, the dogs were treated for 3 days before and 30 days after the procedure with aspirin (325 mg) and dipyridamole (75 mg), except for an initial group of 13 dogs which were treated with warfarin. Minipigs received aspirin (1 mg/kg/day), dipyridamole (3 mg/kg/day), and diltiazem (60 mg/day) on a similar schedule. All procedures were performed using full anticoagulation with heparin (100-200 units/kg).

A series of experiments was also conducted in 36 atherosclerotic rabbits (2-3 kg). Arterial lesions were produced in the aorta (n=5) or iliac arteries (n=31) by balloon catheter deendothelialization and the feeding of a 2% cholesterol, 10% peanut oil enriched diet. Stents were placed at these sites as a secondary intimal injury 6-7 weeks after the initial injury, via carotid arteriotomy and under ketamine/xylazine anesthesia. Heparin (500 units) and placebo (n=15) or aspirin (60 mg, n=21) were given during the procedure; the treatment group continued to receive 60 mg of aspirin every 3 days until sacrifice.

All experimentation was conducted in accordance with federal regulations regarding the care and use of laboratory animals established by the National Institutes of Health, and was performed in such a manner as to minimize stress, pain, and discomfort to the animals. The experimental protocols were approved by the Institutional Animal Care and Use Committees of Emory University and Baylor University.

The stent prosthesis (Fig. 1) consisted of a 0.15 mm diameter stainless steel surgical wire wrapped in a serpentine fashion around a standard angioplasty balloon catheter (with the balloon deflated). After positioning the catheter in the appropriate location within the artery, the balloon was inflated twice to a pressure of approximately 10 atmospheres for 30-60 seconds. This process embedded the stents well within the arterial intima, such that when the balloon was deflated, the catheter was removed leaving the stent in place.

Specimen Fixation and Preparation

For coronary specimens, the heart was quickly excised after anesthetic overdose; the left main coronary artery was then rapidly cannulated. The vasculature was perfused for 2-3 min with oxygenated 0.1 M cacodylate with 4% sucrose (pH 7.4, 317 mOsm) at 100mm Hg pressure and 37° C. This perfusate was also heparinized (10 units/ml). The vasculature was then perfusion fixed for 15 min at 100 mm Hg with oxygenated 2.5% glutaraldehyde in 0.1M cacodylate (pH 7.4, 480 mOsm) at 37° C. The specimens were carefully excised and immersed for 24 h in 2.5% EM grade glutaraldehyde in 0.1 M cacodylate. They were then replaced in 0.1 M cacodylate and kept refrigerated until further processing, usually within one week.

Rabbit aortic and iliac arterial specimens were fixed in situ according to a similar protocol. Under deep pentobarbital anesthesia, a laparotomy was performed and the abdominal aorta and inferior vena cava were cannulated. The

animals were euthanatized by anesthetic overdose, and the buffer and fixative were then perfused as above with efflux via the inferior vena cava.

The stented arterial segments for SEM analysis were trimmed of excess tissue and carefully cut longitudinally with scissors to expose the luminal surfaces. The specimens were postfixed for 1 h in osmium tetroxide (1% in 0.1 M cacodylate, pH 7.4, 344 mOsm) and washed in distilled water to remove any crystalline buffer salts. They were then dehydrated in graded ethanol baths into absolute (100%) and critical point dried from liquid CO_2 using thermoregulation and flow monitoring. After mounting on aluminum stubs, the specimens were sputter coated with 10 nm gold-palladium. The stented arteries were examined on the lower stage of an International Scientific Instruments DS-130 scanning electron microscope in the secondary electron scanning mode at 10kV accelerating voltage. A series of dog and pig coronary specimens were measured for thickness of the intimal covering over the stent wire from SEM micrographs; these data were compared using Student t tests with a Bonferroni correction applied to the level of significance to correct for the total number of t tests performed.

Specimens for light microscopy were embedded in paraffin or Epon after careful removal of the stent wires from 3-5 mm length arterial segments. They were sectioned and stained with hematoxylin and eosin or toluidine blue. A series of rabbit iliac arterial specimens were measured for wall thickness (external elastic lamina to lumen) and lumen diameter using an ocular micrometer; these data were analyzed using analysis of variance.

Specimens for TEM analysis were postfixed in osmium tetroxide (1% in 0.1 M cacodylate) for 1-2 h, washed in distilled water, and dehydrated in graded ethanol baths to 100%. They were then embedded in Epon and sectioned to 70 nm thickness with an LKB ultramicrotome equipped with a diamond knife. The sections were mounted on grids and stained with lead citrate and uranyl acetate. They were examined on a JEOL 100-CX microscope at 80 kV accelerating voltage.

Morphologic Criteria

A list of morphologic documentations of phenomena which were observed associated with arterial stenting was generated. These arterial responses were then assessed semi-quantitatively by assignment of ranking from 0 to 3, depending on severity of the observation in questions per specimen grouping, with 0 = none; 1 = mild; 2 = moderate; 3 = severe. These semi-quantitative measurements were applied for criteria A through H listed below, while either presence (+) or absence (-) of the described morphology was applied for
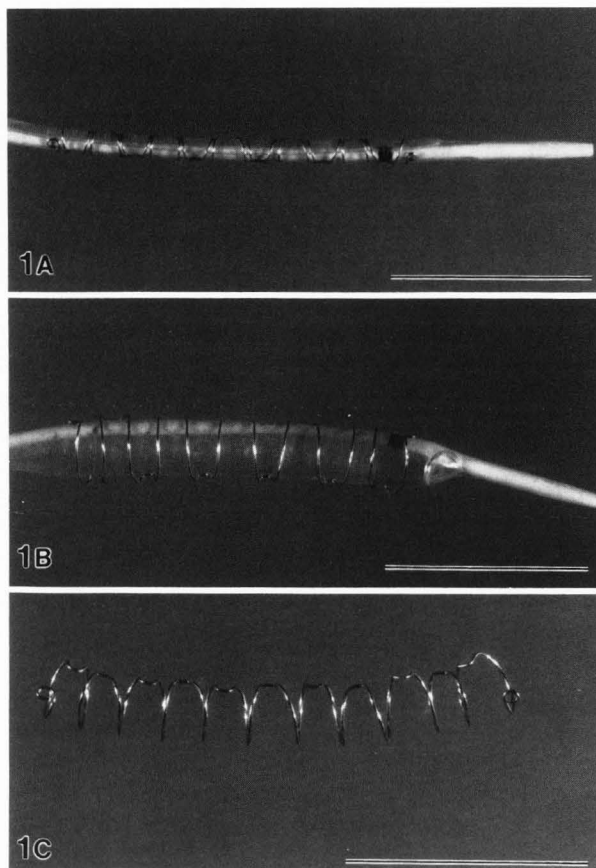
Fig.1. Intravascular stent prosthesis. A) stent mounted on deflated balloon catheter, ready for use; B) wire stent coil is expanded after inflation of balloon; C) coil prosthesis after deflation and removal of balloon catheter. Bars = 10 mm.

criteria I through Q. Listed below are the morphologic criteria and their definitions.

A) Platelet Adhesion: activated platelets adherent to the stent material, damaged endothelium, or exposed subendothelial tissue.

B) Platelet Monolayer: activated platelets adherent not only to the luminal surface or stent material, but also to adjacent platelets, forming a luminal surface covering.

C) Platelet Thrombus: an aggregate of platelets more than one or two cells deep, forming a structure which impinges on the arterial lumen.

D) Fibrin-Erythrocyte Thrombus: a mural or luminal thrombus composed of either fibrinous network, aggregated red blood cells, or both.

E) Leukocyte Adherence: presence of white blood cells other than macrophages on either the luminal tissues or the stent material.

F) Macrophage Adherence: presence of large (> 15 μm diameter) white blood cells with phagocytic morphology on luminal surface or stent material. Such cells displayed spherical or flattened shape, adherent erythrocytes and debris, pseudopodial extensions, and smooth, dimpled, or ruffled plasma membranes.

G) Pseudointima: a luminal surface covering of cells other than endothelial.

H) Endothelial Desquamation: mechanical loss or removal of endothelial cells from the luminal surface of the blood vessel at early time periods as a direct result of stent placement, or at later time periods as a result of arterial wall remodelling.

I) Stellate Endothelial Cells or Pseudoendothelial Cells ((p)EC): presence of periluminal cells with a polygonal or stellate morphology.

J) Elongated (p)EC with Longitudinal Orientation: periluminal cells with elongated morphology, long axis in parallel with direction of blood flow.

K) Elongated (p)EC with Circumferential Orientation: periluminal cells with elongated morphology, but with long axis perpendicular to expected direction of blood flow.

L) Banded (p)EC: periluminal cells with luminal surface ultrastructure suggestive of banded actin cytoskeletal stress fibers (18,47).

M) Perinuclear Microvilli: presence of microvillar protrusions from periluminal cell surface, suggestive of spotted actin cytoskeletal stress elements (18).

N) Luminal (p)EC Openings: Periluminal cells with increased density of luminal surface pits and/or plasmalemma vesicles, suggestive of enhanced endocytosis and/or transcytosis (39,43).

O) Loose (p)EC Junctions: attenuated or incomplete cell-to-cell attachments of periluminal cells.

P) Elaborate (p)EC Junctions: prominent, interdigitated junctional areas of periluminal cells.

Q) Intimal Neovascularity: appearance of endothelial-lined blood vessels within the neointima.

The following criteria were used to characterize intimal cells by TEM. EC were identified by presence at the luminal aspect of the arterial wall as a monolayer of flattened cells with tight and gap junctions, a basal lamina, cytoplasmic Weibel-Palade bodies, and few apical microvilli. SMC were characterized as medial or intimal, spindle-shaped mononuclear cells with a continuous basement membrane, relative abundance of plasmalemmal vesicles, and absence of pseudopodial extensions. SMC were further characterized as contractile or synthetic by the relative content of cytoplasmic

Fig.2. Three days, dog coronary. Light microscopy of paraffin-embedded thick section. The stent wire was removed prior to sectioning leaving a space (*). Thrombus (T) is seen where wire was embedded in the tunica media (TM). L = lumen; IEL = internal elastic lamina. Bar = 50 μm.

Fig.3. Three days, normal minipig coronary. SEM shows stent wire (*) partly embedded in the arterial wall and associated with platelet microthrombi (T). Remnant endothelium (EC) and adherent leukocytes (WBC) are seen; note association of giant cell (GC), adherent to stent wire, and cellular tubelike structures (arrowheads). Bar = 50 μm.

Fig.4. Three days, dog coronary. Higher-power SEM of metallic stent surface (*) which is partially covered by remnant or regenerating tissue to upper left. Platelets (P), fibrin (F), and spreading cells (arrowheads) adhere to stent and tissue. Bar = 10 μm.

Fig.5. Three days, normal minipig coronary. SEM of deendothelialized luminal surface within stented arterial segment; large arrow indicates direction of blood flow. Note remnant endothelium (EC), adherent spheroid cells at right, and spread cells covering surface in left half of micrograph. Arrowheads indicate area depicted in Fig. 6. Bar = 0.1 mm.

microfilaments or rough endoplasmic reticulum, respectively. Leukocytes in the intima were recognized by pseudopodial extensions, cytoplasmic granules, and absence of a basement membrane. Polymorphonuclear leukocytes (neutrophils) were identified by their segmented nuclei and cytoplasmic specific granules. Macrophage-foam cells showed no specific granules, were mononuclear or multinucleated (histiocytes), and had abundant cytoplasmic vacuoles and lysosomes.

Results

An overall assessment of the arterial responses to stenting using the specific morphologic criteria is presented in Table 1.

One Day to One Week

At one to three days after stent placement in all model systems tested, the stent wire was observed partly embedded into the arterial wall and partially covered by thrombus and remnant or regenerating tissue (Figs. 2 and 3). Thrombus associated with the embedded wire and damaged tissue appeared greater in frequency and extent for dog coronary arteries than for rabbit aortas or minipig coronaries. The major thrombic elements
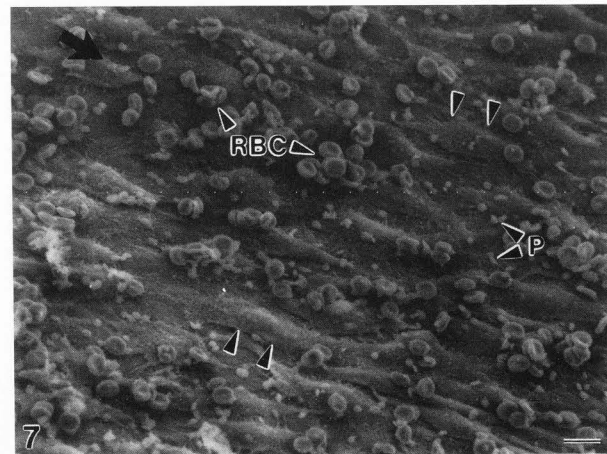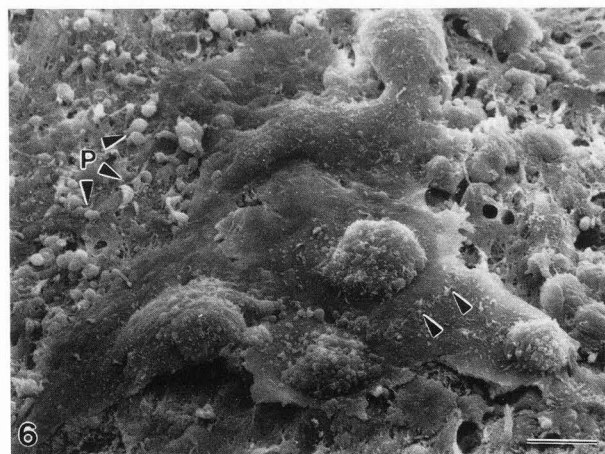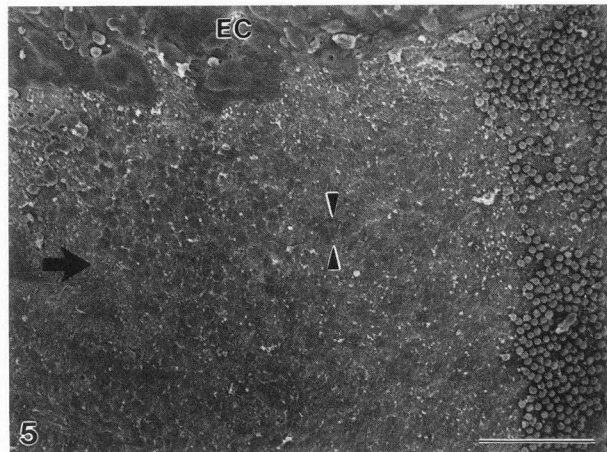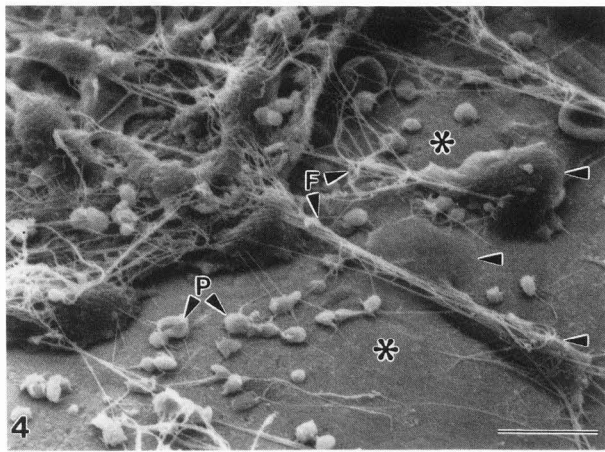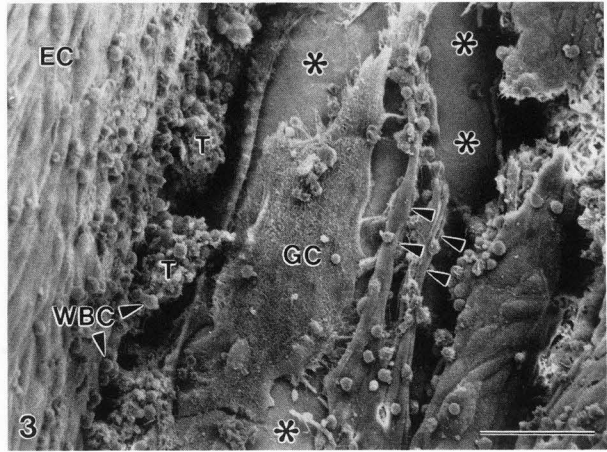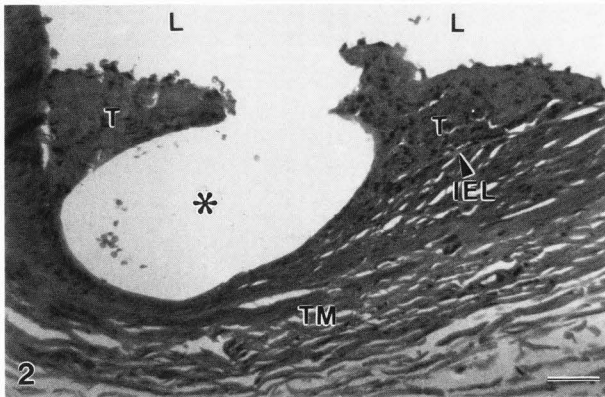
Fig.6. Three days, normal minipig coronary. Platelets (P) and spread cells with prominent nuclear regions, which have formed intercellular attachments (arrowheads), are seen adherent to damaged intima. Bar = 10 μm.

Fig.7. One week, dog coronary. Elongated periluminal cells (arrowheads) show filopodial attachments to damaged intima and adjacent cells. Adherent erythrocytes (RBC) and platelets (P) are also seen. Bar = 10 μm

in dog coronaries were fibrin and erythrocytes, whereas in both rabbits and minipigs, dendritic platelets predominated. In atherosclerotic rabbit aortas one day after stenting, a regular array of spherical and flattened cells was seen adherent to the metal surface of the stent wire (see Ref. 33). Similar cells were observed with decreased frequency at three days in dog and pig coronaries (Fig. 4); a unique feature of the early stent reaction in pig coronaries was the appearance of giant cells of both spheroid and spread shape adherent to the wire prosthesis (Fig. 3).

Areas of endothelial denudation within the stented arterial segments showed primarily a monolayer of dendritic and spread platelets, with occasional platelet thrombi and adherent erythrocytes and fibrin. Adherent leukocytes were frequently observed both in these areas and near the embedded stent wire. Evidence of an early reendothelialization of denuded intima was seen in both normal minipig and dog coronaries, at 3 days and one week, respectively (Figs. 5, 6, and 7). In the minipigs there was apparent spreading of adherent cells to form a monolayer; in the dogs, elongated cells with filopodial cell-cell and cell-substrate attachments were seen. In both cases these features often appeared as islands without a close spatial association to remnant or regenerating EC

sheets.

One Week to Four Weeks

In the one to four week time period, substantial neointimal growth luminal to the stent prosthesis was observed in all models. Complete or nearly complete luminal repaving with endothelial or

---

Fig.8. Ten days, normal minipig coronary. Light microscopy of plastic-embedded thick section. A space (*) is seen where stent wire was embedded in the arerial wall. Thrombus (T) is adjacent to this space, and the internal elastic lamina (IEL) and tunica media (TM) have been disrupted. There is a marked neointimal hyperplasia. L = direction toward lumen. Bar = 50 μm

Fig.9. Ten days, normal minipig coronary. TEM of leukocytes in neointima covering stent. A) macrophage B) polymorphonuclear leukocyte (neutrophil). Bars = 1 μm

Fig.10. Two weeks, dog coronary. Note elaborate cell junctions (J) and longitudinal stress fibers (arrowheads). Bar = 10 μm.

Fig.11. Three weeks, dog coronary. The EC nuclear regions are prominent and display numerous microvilli. There is transverse banding suggestive of stress fibers (arrowheads). Bar = 10 μm.

Table 1. Semiquantitative assessment of SEM observations from animal models of arterial stenting, according to specific morphologic criteria defined in Methods.

Animal Model	Time after Stenting, Days	Total number of SEM Observations	Thrombotic events				Inflammatory events		Periluminal cell events										
			A	B	C	D	E	F	G	H	I	J	K	L	M	N	O	P	Q
Aorta,	0	16	2	1	1	1	2	2	0	3	-	+	-	-	-	+	-	-	-
cholesterol-fed	1	10	2	1	2	1	2	1	0	2	+	+	+	-	+	+	+	-	-
rabbit	7	22	1	0	1	2	2	2	0	2	-	+	+	-	+	+	+	-	-
	14	23	0	0	1	1	1	1	0	1	+	+	+	+	+	+	+	+	-
	28	20	0	0	0	1	1	1	0	0	+	+	+	+	+	-	+	+	-
Coronary artery,	3	24	2	1	1	3	2	1	0	3	-	+	-	-	+	+	-	-	-
dog	7	4	2	2	1	2	1	1	0	2	+	+	+	-	+	-	-	+	-
	14	7	1	0	0	0	1	0	0	2	-	+	+	-	-	-	+	-	-
	28	22	0	0	0	1	0	0	0	0	+	+	-	+	+	+	-	+	-
	180	15	2	2	0	2	1	1	2	2	-	+	-	+	-	-	-	+	+
	360	68	0	0	0	0	1	0	0	0	-	+	-	+	+	+	-	+	+
	540	11	0	0	0	0	1	0	0	0	+	+	-	+	+	-	-	+	-
	720	32	0	0	0	0	0	1	0	0	+	+	+	+	+	-	+	+	+
Coronary artery,	3	64	2	2	1	1	3	3	0	3	-	+	-	-	+	+	-	-	-
pig	10	34	1	0	0	1	2	3	2	1	+	+	+	-	+	+	+	-	-
	30	60	0	0	0	1	2	2	1	1	+	+	-	+	+	+	-	+	+
Coronary artery, cholesterol-fed pig	30	206	1	0	0	1	3	3	2	1	+	+	+	+	+	+	+	+	+
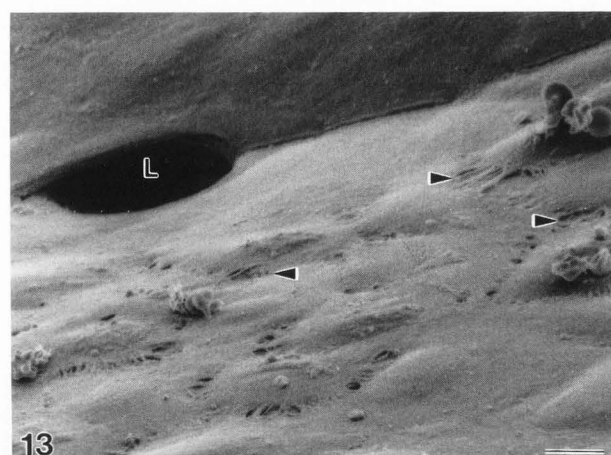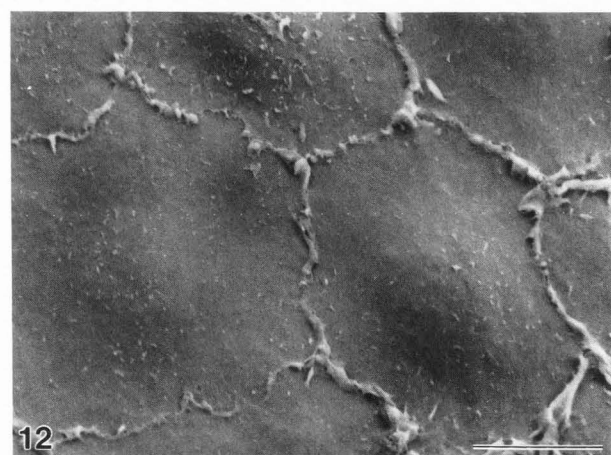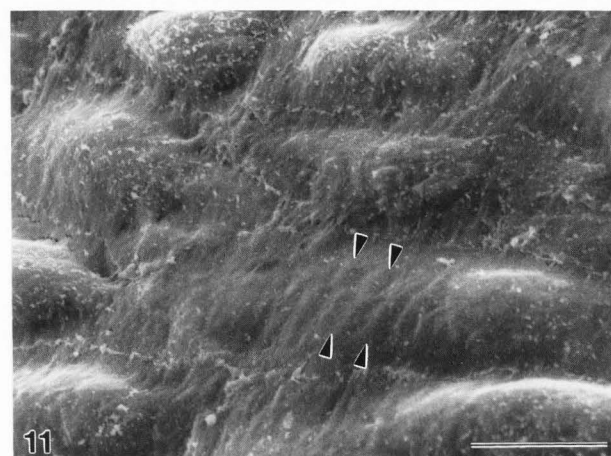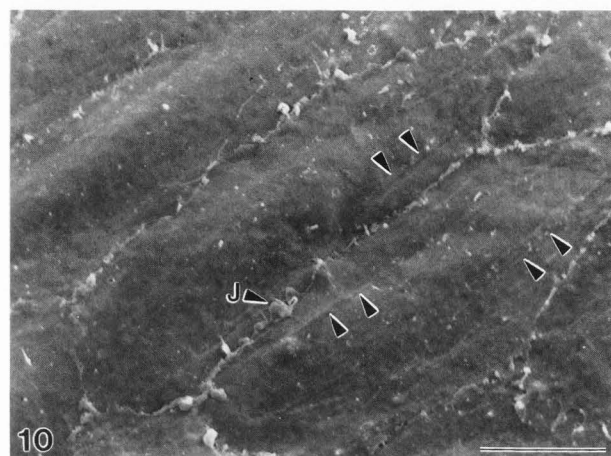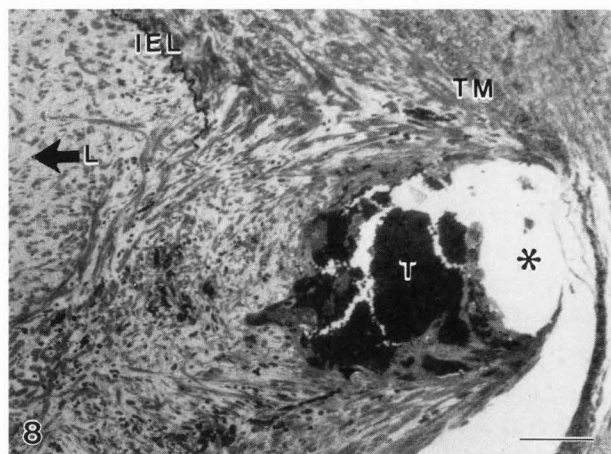
Fig.12. Four weeks, dog coronary. Stellate periluminal cells show complex junctions, surface microvilli, and prominent nuclear regions. Bar = 10 μm.

Fig.13. Four weeks, rabbit aorta. Stellate cells with loose-appearing attachments (arrowheads) near neovascular channel lumen (L). Bar = 10 μm.
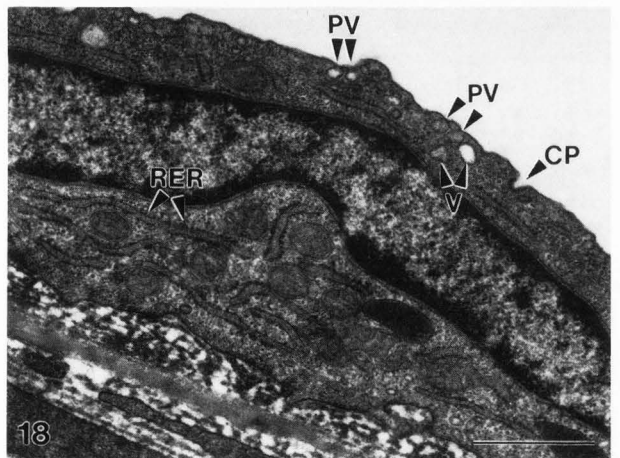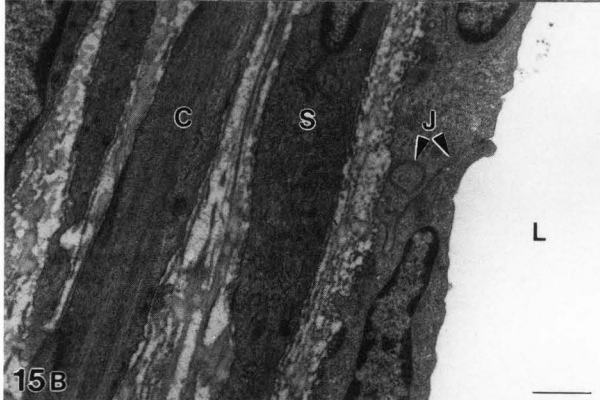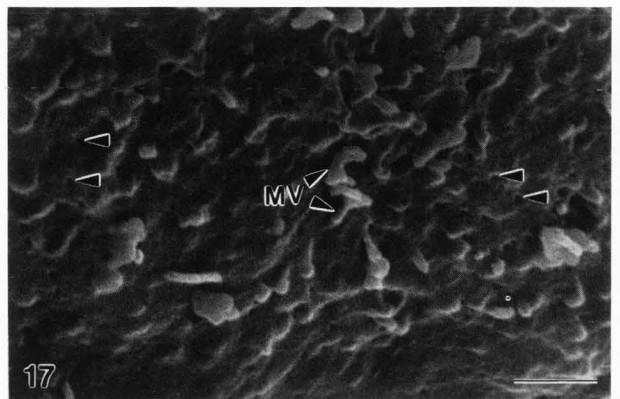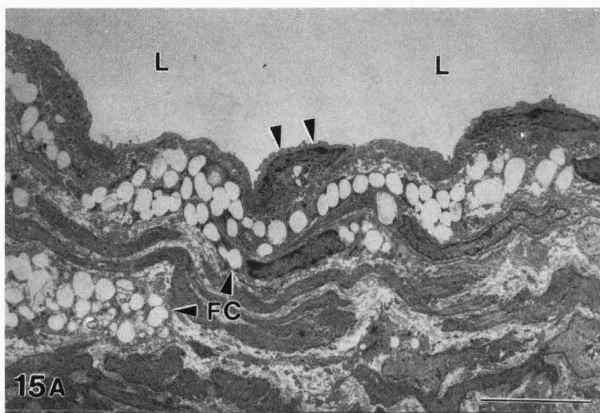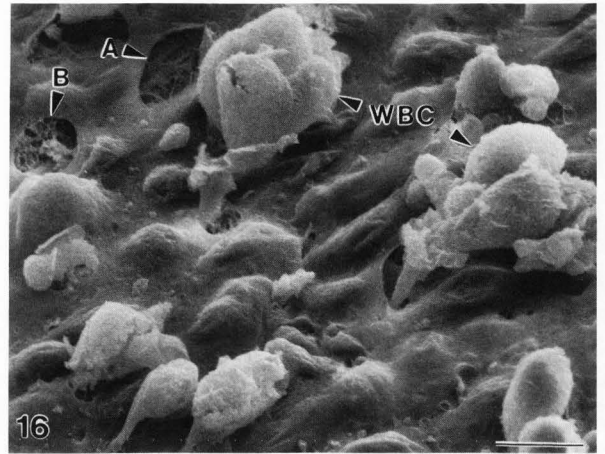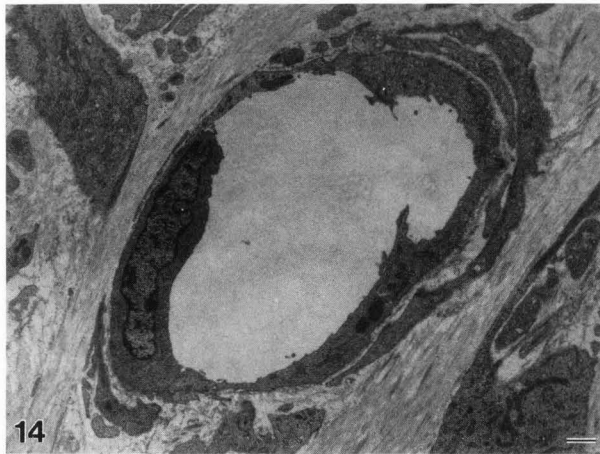
Table 2. Wall thickness (external lamina to lumen) and lumen diameter of iliac arteries four weeks after treatment by angioplasty and stenting or angioplasty alone (control) in aspirin-treated and untreated cholesterol-fed rabbits, measured from hematoxylin and eosin stained thick sections.

	Lumen Diameter mm			Wall Thickness μm	
	Control	Stented		Control	Stented
No aspirin	1.04 ± 0.34	1.45 ± 0.32[a]		262 ± 200	405 ± 217
Aspirin	0.81 ± 0.29	1.26 ± 0.17[b]		532 ± 220	436 ± 145[c]

a = $p < 0.01$ compared to control   b = $p < 0.001$ compared to control   c = $p < 0.05$ compared to control

Fig.14. Thirty days, atherosclerotic minipig coronary. TEM of neovascular channel in neointima covering stent wire. Bar = 1 μm.

Fig.15. TEMs of neointimal tissue. A) Thirty days, atherosclerotic minipig coronary. Subendothelial foam cells (FC) and an EC (arrowheads) with cytoplasmic vacuoles are seen. L = lumen. Bar = 10 μm. B) Thirty days, normal minipig coronary. Note SMCs with contractile (C) and synthetic (S) phenotypes, and interdigitation of EC junction (J). L = lumen. Bar = 1 μm.

Fig.16. Thirty days, atherosclerotic minipig coronary. Leukocytes (WBC) in diapedesis of endothelium. Note discontinuities of endothelium which reveal subendothelial structures with fibrillar (A) and foamy (B) appearances. Bar = 10 μm.

Fig.17. Thirty days, normal minipig coronary. SEM shows numerous EC openings (arrowheads) and microvilli (MV). Bar = 1 μm.

Fig.18. Thirty days, normal minipig coronary. EC shows abundant rough endoplasmic reticulum (RER), cytoplasmic vesicles (V), plasmalemmal vesicles (PV), and a coated pit (CP) by TEM. Bar = 1 μm.

Table 3. Thickness of intimal covering over stent wire in normal and cholesterol-fed minipigs four weeks after stent placement, measured from critical point-dried specimens.

	Normal	Cholesterol-fed
Thickness of intimal covering, μm	278 ± 132	435 ± 176[a]

a = p < 0.001 compared to normal minipigs

Table 4. Thickness of intimal covering over stent wire in dog coronary arteries, measured from critical point dried specimens.

	Time of fixation after stenting, mo.			
	6	12	18	24
Thickness of intimal covering, μm	126 ± 58	81 ± 31	72 ± 32[a]	85 ± 26

a = p < 0.01 compared to 6 month value
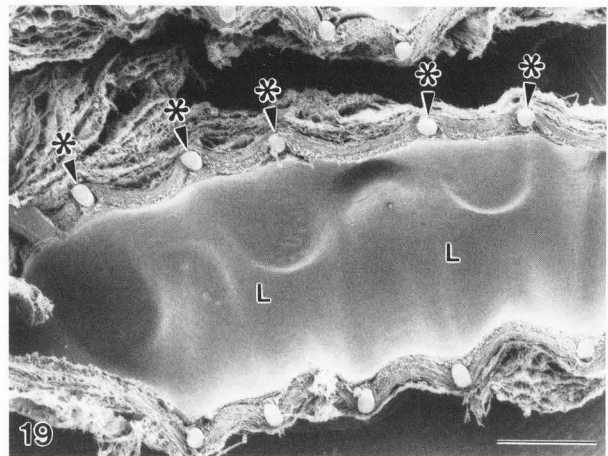
Fig.19. Two years, dog coronary. Low-magnification SEM of entire longitudinal half-section of artery shows stent wire (*) incorporated into arterial wall and covered by a thin neointima. L = lumen. Bar = 1 mm.

pseudoendothelial cells was achieved at 10 days in normal minipigs, two weeks in rabbits, and four weeks in dogs. Scattered adherent microthrombi (primarily fibrin) and leukocytes including macrophages were noted on the luminal surfaces. Light microscopy and TEM revealed the neointima was a form of granulation tissue, composed of thrombic elements, neovascular channels, synthetic SMC, and leukocytes including macrophage foam cells, neutrophils, and histiocytes (Figs. 8 and 9).

The periluminal cells displayed many features suggestive of adaptation to hemodynamic or cytokine stress. These included transverse and longitudinal banding, complex junctional areas, and apical microvilli (Figs. 10 and 11). Some specimens showed an endothelial or pseudoendothelial layer which was immature or undifferentiated as evidenced by stellate cell shape (forming the "cobblestone" appearance of EC in confluent culture), prominent nuclear areas, and attenuated or complex intercellular attachments (Figs. 12 and 13).

Morphometric analysis was performed on iliac artery specimens from atherosclerotic rabbits, perfusion fixed 4 weeks after randomized treatment of the preexisting bilateral stenoses by either balloon angioplasty alone or angioplasty plus stenting. Stenting after balloon dilatation resulted in significantly larger luminal diameter whether or not the animals were treated with aspirin, and for aspirin treated rabbits, stenting led to a slight but significant decrease in arterial wall thickness (Table 2). The stent wires were enclosed in a neointimal cell layer composed of foam cells and spindle-shaped cells with an abundant extracellular matrix (see Ref.33). Late fibrotic subtotal occlusion of the stent occurred in two animals not treated with aspirin.

Four Weeks to Two Years

Coronary arteries of both normal and atherosclerotic miniature swine were examined at 30 days after stent placement.

Thickness of the neointimal covering of the prosthesis was significantly greater for cholesterol-fed minipigs compared to those fed a diet of standard chow (Table 3). Macrophage-foam cells and lipid-laden SMC were observed more frequently in specimens from atherosclerotic compared to normal swine, as were neovascular channels (Figs. 14 and 15). SEM of the luminal surfaces showed a confluent cell layer with endothelial-like morphology, but with frequent histologic and ultrastructural abnormalities seen in both groups. These included the formation discontinuities in the EC layer (Fig. 16), necrosis and sloughing of entire cells, absent or oddly-shaped Weibel-Palade bodies, leukocytes undergoing diapedesis of the endothelium (Fig. 16), adherent microthrombi, and increased density of luminal surface openings and microvilli (Figs. 17 and 18). Two specimens from the atherosclerotic groups showed luminal surfaces which were predominantly pseudointimal, with erythrocytes and foam cells embedded in a fibrous matrix.

Examination of long-term stented dog coronary arteries showed coverage of the prosthesis by a thin neointima of spindle-shaped cells with abundant collagen. The thickness of this layer did not progress from 6 months to 2 years (Table 4 and Fig. 19). The EC primarily showed normal morphology, with elongation and flow-directed orientation, but areas over the stent wire occasionally exhibited stellate cells with loose or complex junctions and leukocyte adherence.

Discussion

This study demonstrates the utility of SEM and correlative microscopies for the investigation of arterial responses to stent prosthesis implantation, as has been previously shown in other fields of clinical research (21). Furthermore, it underscores the importance of delicate specimen handling and preparation techniques for the determination of these responses. Finally, it has established the salient morphologic features of vascular histologic reactions in several animal models, providing insights into processes which might reasonably be expected to occur with the application of this device in human coronary and peripheral arteries.

Some of the EC responses to stenting such as the appearance of luminal discontinuities and surface microvilli have also been shown to occur with deviations from standard specimen preparation procedures such as low oxygen tension of the perfusate (32) as well as with pathophysiologic mechanisms including cytokine or fluid shear stress exposure (5,18,47), in surgical clamp ischemia (19), and in experimental atherosclerosis

(34,39,43). In addition, the influence of specimen preparation technique on morphometric analysis of blood vessels is also well known (22). Thus it is crucial to apply appropriate perfusion fixation and delicate specimen handling to insure the validity of ultrastructural observations. These procedures include proper pH and osmolarity of buffer and fixative, temperature and oxygenation considerations, brief exposure to buffer before fixation, postfixation osmication, and slow transition through the critical point during drying. The assessments of ultrastructural features made in this study, therefore, are of physiological relevance because of the application of these procedures.

A common finding among all the models used in this investigation was that thrombus deposition was primarily localized to areas in which the stent wire was embedded in the tissue; the animal showing the most severe thrombosis was the dog. The only thrombotic occlusions that occurred were two instances in the initial series of dog coronary implantations, in which warfarin was used as an anticoagulant, and two instances in the rabbit iliac artery in which the animals were not pretreated with aspirin. Acute patency of this and other stent designs even in the absence of prolonged anticoagulation has been established in various animal models by a number of investigators (10,33,36,37,38,49, and Rodgers, G., manuscript in preparation). Inhibition of stent thrombosis has been shown using a combination of heparin, aspirin, dipyridamole, and dextran (37), and with intravenous administration of a synthetic surface active copolymer, poloxamer 188 (Robinson, K., manuscript in preparation). The process of stent implantation by expansion via balloon catheter appears to embed the prosthesis well into the vascular wall, largely removing the thrombogenic stainless steel from exposure to the circulating blood. It is probable that once the acute phase of thrombosis is complete, there is a reduced likelihood of thrombotic occlusion due to coating of the exposed metal by serum proteins, combined with localized release of fibrinolytic and antithrombotic tissue elements (25,48). However, the presence of mural thrombi can influence the subsequent extent of intimal hyperplasia by at least three mechanisms.

First, the thrombus is a nidus into which activated smooth muscle cells of the arterial wall, as well as blood-borne cells, can migrate and proliferate. Second, platelet-derived growth factor and other granule contents such as serotonin released from platelets of mural thrombi are involved in the regulation of myocyte and fibroblast replication (35). Finally, macrophages and other leukocytes attracted

to the stented region by chemotactic factors from damaged tissue, complement activation on the foreign body, and the thrombic elements themselves, become incorporated into the thrombi and contribute to regulation of fibrous hyperplasia (6,14,23,25,44).

An inflammatory reaction to stent placement, as determined by the presence of cells morphologically characterized as leukocytes both on the luminal surface and in the intima, was present but variable between the three animal models and appeared greater in extent in the cholesterol fed rabbits and minipigs. Neutrophils and monocytes are probably first attracted to the stented region by complement factors activated via the alternate pathway on the stainless steel surface, platelet-released substances, and fibrinopeptides (25). Macrophages then appear by differentiation from circulating monocytes. Macrophages are known to produce chemotactic and angiogenic substances as well as factors mitogenic for fibroblasts, SMC, and EC and may therefore play a pivotal role in the regulation of intimal regrowth over the prosthesis (6,23,42,44), as has been demonstrated in lactide-glycolide copolymer absorbable grafts (11). It is of interest that thrombosis, luminal leukocyte and macrophage adherence, foam cell formation in the intima, the appearance of neovascular channels, excessive intimal thickening, and deviations from normal EC morphology were all observed primarily in close proximity to areas of stent wire embedding. This suggests a complex interrelation of the cellular elements involved in the biologic reaction to the prosthesis, which like the restenosis phenomenon itself, essentially resembles a wound healing reaction (2).

An endothelial-like morphology was exhibited by the regenerated periluminal cell layer in most of the long term stented specimens. However, in many areas features were observed which suggest either phenotypic heterogeneity (induced by hemodynamic or cytokine stresses, or by the initial injury (16)), or an origin other than endothelial. These features included absence of Weibel-Palade bodies by TEM, and by SEM polygonal morphology, loose or complex cell-to-cell attachments, adherent microthrombus and leukocytes, giant cell formation, and circumferential long axis orientation. In arteries stripped of endothelium in vivo by balloon catheter, two distinct populations of regenerated periluminal cells have been identified: endothelial cells and modified smooth muscle cells (31,42,47). Luminal repopulation with endothelial cells proceeds rapidly in rat aortae from the edges of undamaged tissue (pannus ingrowth) as well as from branch ostia, and is associated with reduced intimal thickening (17,43).

Studies in the arterialization of vascular grafts may also provide information about cellular responses to stenting. While some investigators have maintained that the only sources of EC and SMC lining prostheses are from pannus ingrowth and (in porous prostheses) transmural capillary ingrowth (7,8), others have suggested and demonstrated that multipotent, undifferentiated circulating cells can contribute to endothelial-and smooth muscle-like growth (11,15,27,29). Our observations of early luminal repopulation (Figs. 5,6, and 7) lend support to this concept. With regard to stenting, it is likely that primary placement of the device in previously undamaged vessels leaves behind a population of remnant endothelial cells sufficient to cover the prosthesis. However, two of the models reported here (atherosclerotic rabbit and minipig) involved previous deendothelialization of the stented site, and all used balloon angioplasty immediately prior to stenting to mimic as closely as possible the clinical setting. These procedures may increase the likelihood of luminal cells originating from lines other than endothelial, since the proliferative capacity of the EC may be limited.

The regenerated periluminal cell layer of stented arteries could arise from three sources, including 1) endothelium proximal and distal to the stent, from branch vessels, and from remnant patches within the stent; 2) smooth muscle from the tunica media; and 3) undifferentiated circulating cells. These cells may demonstrate endothelial-like morphology while lacking important functions such as production of prostacyclin and heparin-like SMC growth inhibitor, selective permeation of circulating macromolecules, and regulation of vascular tone. Identification of the origin and functions of this and other cell types involved in the tissue reaction to stent placement can only be inferred from the present study and will require the application of immunocytochemical techniques.

A final feature of the arterial response to stenting which was observed in all animal models, as well as with the application of other stent designs by a number of investigators, is atrophy of the tunica media (10,37,38,49). This phenomenon may be related to either reduced exposure of smooth muscle to arterial pulsatile blood flow by the scaffold-like support of the prosthesis, or to mechanical compression with thinning and necrosis. The attenuation of the media was apparent even in acutely stented specimens favors the latter explanation, although both mechanisms may be operative. As with other responses, medial atrophy was observed primarily in areas adjacent

to stent wire embedding, whereas the media in areas distant from the stent appeared normal.

Although these results represent an initial experience with a prototypic device, they are encouraging and it is hoped that informed aggressiveness in stent technology and research will lead to improvements with clinical benefit. While stents have been shown to function well as "bail-out" devices in cases of failed angioplasty, the long term effects in large patient sample populations are as yet unknown. Thus, whether this mechanical approach to post-angioplasty restenosis will be at once safe, efficacious, and of clinical value remains an unanswered question. Concurrently, technical advances to enhance materials and design features should be sought. For example, stents of absorbable materials have undergone preliminary testing (Slepian M., work in progress) and the concept of bonding or coating stents with biologically active substances has been suggested (20). Engineering and biomaterials technology should be applied towards these goals.

In summary, the balloon catheter expandable, wire coil stent was placed largely free of acute thrombotic events in four animal models. Mild to moderate localized thrombus deposition followed by thrombus organization, medial atrophy, neointimal hyperplasia, and (pseudo-)endothelialization led to prosthesis incorporation largely free of late fibrotic stent closures. The cellular events documented here suggest that 1) stents may be incorporated into human arteries by similar mechanisms, and 2) antithrombotic, anti-inflammatory, and antimitotic drugs may be useful for reducing both the hyperplastic response to stenting and the threat of acute thrombotic closure. Further research should be directed toward 1) characterization of functional cellular responses to stenting, 2) improvement in stent technology, and 3) pharmacologic approaches to enhance stent safety and efficacy.

Acknowledgements

References

1. Apkarian R, Burns J, Acland R. (1982). Scanning electron microscopic study of disturbances in arterial walls following microsurgical needle perforations. Scanning Electron Microsc 1982;II:781-787.

2. Austin G, Ratliffe N, Hollman J, Tabei S, Phillips D. (1985). Intimal proliferation of smooth muscle cells as an explanation for recurrent coronary artery stenosis after percutaneous transluminal coronary angioplasty. J Am Coll Cardiol 6:369-375.

3. Block P, Baughman K, Pasternak R, Fallon J. (1980). Transluminal angioplasty: correlation of morphologic and angiographic findings in an experimental model. Circulation 61(4):778-785.

4. Block P, Myler R, Stertzer S, Fallon J. (1981). Morphology after transluminal angioplasty in human beings. N Engl J Med 305(7):382-385.

5. Bucana C, Trial J, Papp A, Wu K. (1988). Bovine aorta endothelial cell incubation with interleukin 2: morphological changes correlate with enhanced vascular permeability. Scanning Microsc 2(3):1559-1566.

6. Clark R. (1988). Overview and general considerations of wound repair. In Clark R, Henson P, (eds.). The Molecular and Cellular Biology of Wound Repair. Plenum Press, New York, pp 3-23.

7. Clowes A, Gown A, Hanson S, Reidy M. (1985). Mechanisms of arterial graft failure: 1) role of cellular proliferation in early healing of PTFE prostheses. Am J Pathol 118:43-54.

8. Clowes A, Kirkman T, Reidy M. (1986). Mechanisms of arterial graft healing: rapid transmural ingrowth provides a source of intimal endothelium and smooth muscle in porous PTFE prostheses. Am J Pathol 123:220-230.

9. Dotter C, Judkins M. (1964). Transluminal treatment of arteriosclerotic obstruction: description of a new technique and a preliminary report of its application. Circulation 30:654.

10. Dotter C, Buschmann R, McKinney M, Rosch J. (1983). Transluminal expandable nitinol coil stent grafting: preliminary report. Radiology 147:259-260.

11. Griesler H, Dennis J, Endean E, Ellinger J, Buttle K, Kim D. (1988). Derivation of neointima in vascular grafts. Circulation 78(Suppl I):I6-I12.

12. Gruentzig A, Senning A, Siegenthaler W. (1979). Non-operative dilatation of coronary artery stenoses: percutaneous transluminal coronary

angioplasty. N Engl J Med 301:61.

13. Guidoin R, Marois M, Martin L, Blais P, Laroche F, Noel H. (1979). The processed human umbilical vein as an arterial substitute: evaluation in canine models and case report on human implantation. Scanning Electron Microsc 1979;III:843-850.

14. Guyton J, Karnovsky M. (1979). Smooth muscle cell proliferation in the occluded rat carotid artery: lack of requirement for luminal platelets. Am J Pathol 94:585-602.

15. Harker L, Schlichter S, Sauvage L. (1977). Platelet consumption by arterial prosthesis: the effects of endothelialization and pharmacologic inhibition of platelet function. Ann Surg 186:594-601.

16. Haudenschild C, Grunwald J. (1985). Proliferative heterogeneity of vascular smooth muscle cells and its alteration by injury. Exp Cell Res 157:364-370.

17. Haudenschild C, Schwartz S. (1979). Endothelial regeneration: restitution of endothelial continuity. Lab Invest 41(5):407-418.

18. Herman I, Brant A, Warty V, Bonasccorso J, Klein E, Kormos R, Borovetz H. (1987). Hemodynamics and the vascular endothelial cytoskeleton. J Cell Biol 105:291-302.

19. Kawamura J, Sunaga T, Mulhern L, Nelson E. (1973). Ischemia of the common carotid artery in rabbits: scanning and transmission electron microscopy of the luminal surface. Scanning Electron Microsc 1973:465-472.

20. King S. (1988). Vascular stents and atherosclerosis (editorial). Circulation 79:460-462.

21. Laschi R, Pasquinelli G, Versuna P. (1987). Scanning electron microscopy application in clinical research. Scanning Microsc 1(4):1771-1795.

22. Lee R. (1987). Preservation of in vivo morphology of blood vessels for morphometric studies. Scanning Microsc 1(3):1287-1293.

23. Leibovitch S, Ross R. (1976). A macrophage-dependent serum factor that stimulates the proliferation of fibroblasts in vitro. Am J Pathol 84:304-314.

24. Leimgruber P, Roubin G, Hollman J, Cotsonis G, Douglas; J, King S, Gruentzig A. (1986). Restenosis after successful coronary angioplasty in patients with single-vessel disease. Circulation 73:710-717.

25. Leonard E, Turrito V, Vroman L (eds.), (1987). Blood in contact with natural and artificial surfaces. Annals New York Acad Sci 516:306-313.

26. Mackenzie D, Hackett M, Tibbs D. (1968). Origin of arterial prosthesis lining from circulating blood cells. Arch Surg 97:879-885.

27. McAuslan B, Hannan G, Reilly W. (1982). Signals causing change in morphologic phenotype, growth mode, and gene expression of vascular endothelial cells. J Cell Physiol 112:96-106.

28. Mehdorn H, Townsend J, Weinstein P, Chater N, Meyerman R, Buncke H. (1979). Endothelialization of a new microvascular graft material. Scanning Electron Microsc 1979;III:851-856.

29. O'Neal R, Jordan G, Rabin E, DeBakey M, Halpert B. (1964). Cells grown on isolated intravascular Dacron hub: an electron microscopic study. Exp Mol Path 3:408-422.

30. Pasquinelli G, Preda P, Curti T, D'Addato M, Laschi R. (1987). Endothelialization of a new dacron graft in an experimental model: light microscopy, electron microscopy, and immunocytochemistry. Scanning Microsc 1(3):1327-1338.

31. Reidy M, Clowes A, Schwartz S. (1983). Endothelial regeneration: inhibition of endothelial regrowth in arteries of rat and rabbit. Lab Invest 49(5):569-575.

32. Richardson M, Parbtani A. (1987). Identification of non-denuding endothelial injury by scanning electron microscopy. Scanning Microsc 1(3):1315-1326.

33. Robinson K, Roubin G, Siegel R, Black A, Apkarian R, King S. (1988). Intra-arterial stenting in the atherosclerotic rabbit. Circulation 78:646-653.

34. Rodman N, Jagganathan S, Jenkins J, Rodman J, Allender P. (1979). Experimental atherosclerosis: surface ultrastructural studies in the rabbit aorta. Scanning Electron Microsc 1979;III:835-841.

35. Ross R, Glomset J, Kariya B, Harker L. (1974). A platelet-dependent serum factor that stimulates the proliferation of arterial smooth muscle cells in vitro. Proc Nat Acad Sci 71(4):1207-1210.

36. Roubin, G, Robinson K, King S, Gianturco C, Black A, Brown J, Siegel R, Douglas J. (1987). Acute and late results of intracoronary stenting after coronary angioplasty in dogs. Circulation 76(4):891-897.

37. Schatz R, Palmaz J, Tio F, Garcia F, Garcia O, Reuter S. (1987). Balloon-expandable intracoronary stents in the adult dog. Circulation 76(2):450-475.

38. Sigwart U, Pyel J, Mirkovitch V, Joffre F, Kappenberger L. (1987). Intravascular stents to prevent occlusion and restenosis after transluminal angioplasty. N Engl J Med 316:701-706.

39. Simionescu N. (1988). Prelesional changes in atherogenesis. In Simionescu N, Simionescu M (eds.), Endothelial Cell Biology in Health and

Disease. Plenum Press, New York, pp 385-429.

40. Steele P, Chesebro J, Stanson A, Holmes D, Dewanjee M, Badimon L, Fuster V. (1985). Balloon angioplasty: natural history of the pathophysiologic response to injury in a pig model. Circ Res 57:105-112.

41. Stemerman M, Spaet T, Pitlick F, Cintron J, Lejnieks I, Tiell M. (1977). Intimal healing: the pattern of reendothelialization and intimal thickening. Am J Pathol 87:125-142.

42. Taylor K, Scaffer T, Wisler R, Glagov S. (1979). Immuno-morphologic identification and characterization of cells derived from experimental atherosclerotic lesions. Scanning Electron Microsc III:815-822.

43. Trillo A, Prichard R. (1979). Early endothelial changes in experimental primate atherosclerosis. Lab Invest 41:294-302.

44. Verheyen A, Vlaminckx E, Lauwers F, Saint-Guillain M, Boergers M. (1988). Identification of macrophages in intimal thickening of rat carotid arteries by cytochemical localization of purine nucleoside phosphorylase. Arteriosclerosis 8:759-767.

45. Waller B, McManus B, Gorfinkel J, Kishel J, Schmidt E, Kent K, Roberts W. (1983). Status of the major epicardial coronary arteries 80 to 150 days after percutaneous transluminal coronary angioplasty: analysis of 3 necropsy patients. Am J Cardiol 51:81-84.

46. Webster W, Bishop S, Geer J. (1974). Experimental aortic intimal thickening: endothelialization and permeability. Am J Pathol 76:265-284.

47. White G, Fujiwara K. (1986). Expression and intracellular distribution of stress fibers in aortic endothelium. J Cell Biol 103:63-70.

48. Wolf H, Karwath R, Groth T. (1988). Interaction of blood with biomedical polymers: basic aspects. In: Advances in Biomedical Measurement. Plenum Press, New York, pp 133-142.

49. Wright K, Wallace S, Charnsangavej C, Carrasco C, Gianturco C. (1985). Percutaneous endovascular stents: an experimental evaluation. Radiology 156:69-72.

50. Zollikofer C, Chain J, Salomonowitz E, Runge W, Bruehlmann W, Castaneda-Zuniga W, Amplatz K. (1984). Percutaneous transluminal angioplasty of the aorta: light and electron microscopic observations in normal and atherosclerotic rabbits. Radiology 151:355-363.

Discussion with Reviewers

U. Sigwart: For how long were the miniature swine and atherosclerotic rabbits fed with atherogenic diet?
Authors: Miniature swine were fed the diet for 2 weeks before the primary arterial injury and until sacrifice. The rabbits were fed for one week before the initial injury until sacrifice.

M. Richardson: What are "flaps" of arterial intima?
Authors: When an atherosclerotic stenosis is dilated by balloon catheter angioplasty, the lumen is enlarged primarily by stretching of the media and adventitia, with fracture and separation of the diseased intima. It is this separated plaque which forms the intimal flap (see Fig.20). Flaps are probably formed to some extent in all balloon-dilated diseased vessels, but when very large flaps are created, acute closure can result.
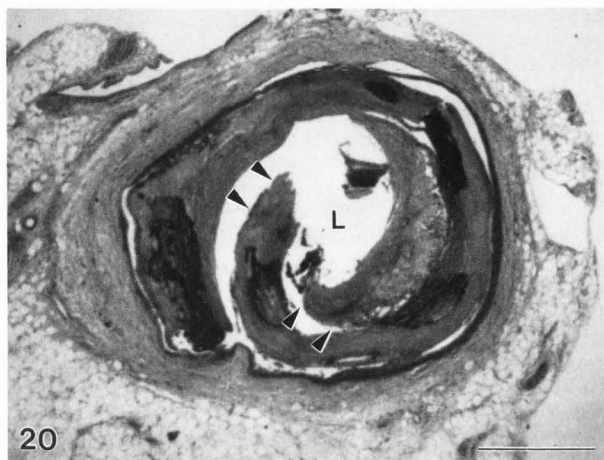
Fig.20. Light microscopy of paraffin-embedded thick section stained with hematoxylin and eosin. Specimen is coronary artery from patient who died suddenly 6 h after balloon angioplasty. Intimal flaps (arrowheads) created by fracture and dehiscence of atherosclerotic intima impinge on lumen (L). Bar = 1 mm.

R. Laschi: Do you have data supporting the view that intravascular stents really improve some hemodynamic factors?
Authors: We have not as yet systematically evaluated hemodynamic factors with the application of this stent. However, anecdotal evidence suggests a reduction in the post-angioplasty transstenotic blood pressure gradient after stenting for vessels with postprocedural closure. Puel and colleagues found that stenosis geometry was further improved by stenting immediately after angioplasty, using an intracoronary stent of a different design (Puel J, Bertrand M, Rickards A, Sigwart U, Serruys P. (1988). Early and late assessment of stenosis geometry after coronary arterial stenting. Am J Cardiol

61:546-553). Minimum luminal cross-sectional area and obstruction diameter were increased, and stenotic percent area and percent diameter were decreased; these changes were associated with decreased turbulent and Poiseuillian resistance, as well as decreased theoretical transstenotic pressure gradient.

R. Laschi: Did you observe any foreign body reaction against your stent device?
Authors: The inflammatory and fibrotic responses which we observed could be considered a generalized foreign-body reaction, since they would not have occurred were the prosthetic foreign material not introduced. A specific giant cell foreign-body reaction, however, was consistently seen only in the pig coronaries.